Earth and Planetary Science Letters 542 (2020) 116296

Contents lists available at ScienceDirect

Earth and Planetary Science Letters

www.elsevier.com/locate/epsl

Pūhāhonu: Earth's biggest and hottest shield volcano

Michael O. Garcia [a,*], Jonathan P. Tree [a], Paul Wessel [a], John R. Smith [b]

[a] Department of Earth Sciences, University of Hawai'i at Mānoa, Honolulu, HI 96822, USA
[b] Department of Oceanography, University of Hawai'i at Mānoa, Honolulu, HI 96822, USA

ARTICLE INFO

Article history:
Received 22 November 2019
Received in revised form 5 April 2020
Accepted 18 April 2020
Available online xxxx
Editor: R. Dasgupta

Keywords:
Hawaii
volume
gravity
olivine
magma temperature
solitary wave

ABSTRACT

New bathymetric and gravity mapping, refined volume calculations and petrologic analyses show that the Hawaiian volcano Pūhāhonu is the largest and hottest shield volcano on Earth. This ~12.5-14.1 Ma volcano in the northwest Hawaiian Ridge (NWHR) is twice the size of Mauna Loa volcano (148 ± 29 vs. 74.0×10^3 km^3), which was assumed to be not only the largest Hawaiian volcano but also the largest known shield volcano. We considered four testable mechanisms to increase magma production, including 1) thinner lithosphere, 2) slower propagation rate, 3) more fertile source, and 4) hotter mantle. The first three of these have been ruled out. The lithosphere was old (~88 Myrs) when Pūhāhonu was formed, and thus, too thick and cold to allow for greater extents of partial melting. The propagation rate was relatively fast when it erupted (87 km/Myr), so this is another unlikely reason. Source fertility was Kea-like and no more fertile than for other much smaller NWHR volcanoes. A hotter mantle remains the best mechanism to produce the large magma volumes and is consistent with the high forsteritic olivine phenocryst compositions (up to 91.8%) and the calculated high percent of melting (24%). Thus, the gargantuan size of Pūhāhonu reflects its high melting temperature, the highest reported for any Cenozoic basalt. A solitary wave within the Hawaiian plume is the probable cause of Pūhāhonu's higher melting temperature and the resulting increased volume flux given the absence of a more fertile source for Pūhāhonu basalts, as found for many basalts from the Hawaiian Islands.

1. Introduction

Recent bathymetric mapping of the Papahānaumokuākea Marine National Monument (PMNM) that includes the southern two-thirds of the Northwest Hawaiian Ridge (NWHR) has revealed the complexity and diversity of the volcanoes within this previously poorly studied section of the Hawaiian-Emperor Chain (Fig. 1). The Hawaiian-Emperor Chain is the classic and best studied example of a string of volcanoes formed by a mantle plume (e.g., Morgan, 1971), although we are continuing to discover new insights into its evolution (e.g., Jicha et al., 2018). The Chain spans ~6000 kilometers with >120 volcanoes that erupted over the past ~82 million years (e.g., Jackson et al., 1972; Clague, 1996). It is subdivided into three segments: from older to younger, the Emperor Seamounts, the NWHR, and the Hawaiian Islands. The NWHR, the focus of this study, spans ~2800 kilometers between the bend in the Hawaiian-Emperor chain and the Hawaiian Islands. At least 52 Cenozoic volcanoes formed within the NWHR over ~42 million years (e.g., Garcia et al., 2015; Jicha et al., 2018). These volcanoes are diverse in shape but generally are less voluminous than those from the Hawaiian Islands (Fig. 1), with the notable exception of Pūhāhonu (Bargar and Jackson, 1974).

The isolation of the NWHR in the central north Pacific basin resulted in it being relatively poorly mapped until recent marine surveys that were organized to characterize the PMNM. These new surveys provided bathymetric details for reinterpreting the geologic history of the NWHR (Kelley et al., 2015). Here we focus on Pūhāhonu (its surface expression is also called Gardner Pinnacles), which was once considered the largest volcano in the Hawaiian-Emperor Chain based on low-resolution bathymetry (54×10^3 km^3; Bargar and Jackson, 1974). Two barren small rocky islands (0.024 km^2) at 25°N, 168°W are the only remnants of the once majestic Pūhāhonu volcano. These "pinnacles" (rising up to 52 m above sea level) are the westernmost subaerial volcanic rocks in the HE Chain. They form a distinctive landmark that Hawaiians named Pūhāhonu ("turtle surfacing for air"). The first documented sighting of the pinnacles was in June 1820, by the American whaler *Maro* (Clapp, 1972) ~1000 km northwest of Honolulu, Hawai'i (Fig. 1). The first recorded landing on Pūhāhonu occurred in March 1828, when crew from the Russian vessel *Moller* went ashore. Pūhāhonu was included in the 'Hawaiian Islands Bird Reservation' by Exec-

* Corresponding author.
E-mail address: mogarcia@hawaii.edu (M.O. Garcia).

https://doi.org/10.1016/j.epsl.2020.116296
0012-821X/

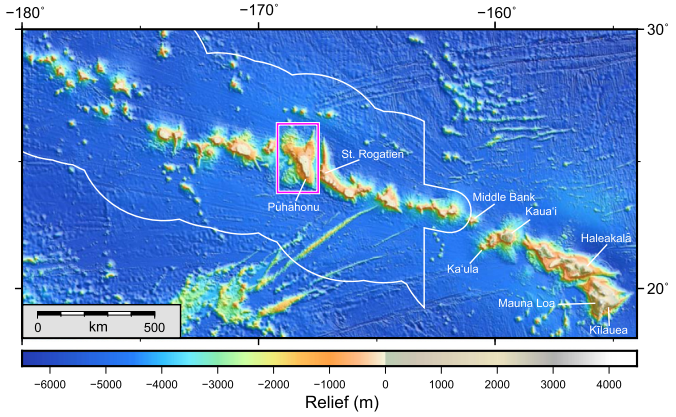

Fig. 1. Map of the Northwest Hawaiian Ridge and Hawaiian Islands. White polygon shows the current PMNM boundary. Magenta box shows the location of Fig. 2. The map is based on SRTM15+V2 elevation data from Tozer et al. (2019). (For interpretation of the colors in the figure(s), the reader is referred to the web version of this article.)

utive Order 1019 of President Theodore Roosevelt in 1909 (Clapp, 1972). It is now part of the PMNM.

2. Previous sampling of Pūhāhonu

Twelve highly altered lavas were collected from the pinnacles in 1971 (Dalrymple et al., 1974). The volcano was dredged in 1972 and 1976 by the University of Hawai'i, and twice in 1984 by the U.S. Minerals Management Service (Fig. 2). The petrography, and major and trace element composition of weakly altered rocks from these dredges indicates they are alkalic and tholeiitic basalts (Garcia et al., 2015). Three of these samples, one tholeiite (from the 1976 dredge haul, 76-6-7) and two weakly alkalic basalts (from the 1972 dredge haul, 72-37), were dated by K/Ar methods yielding an average age of 12.3 ± 2.0 Ma (Garcia et al., 1987). A tholeiitic lava from the 1976 dredge haul yielded a $^{40}Ar/^{39}Ar$ plateau age of 14.11 ± 0.16 Ma (Jicha et al., 2018). One sample from the 1976 dredge haul and two from the 1984 dredge hauls were also analyzed for trace elements, and Pb, Sr and Nd isotopes (Harrison and Weis, 2018). Six tholeiitic lavas from the 1976 dredge haul (including the dated lava) were studied here. They are nearly identical petrographically with sparse vesicles (~1-2 vol.%) and abundant (15-24 vol.%), fresh olivine phenocrysts (>0.5 mm across). These rocks have 12-17 wt% MgO and whole-rock Mg#'s [100(Mg/Mg + Fe^{2+})] of 68-74 (assuming 90% of total iron is Fe^{2+}; Garcia et al., 2015).

3. Methods

3.1. Volume calculations and gravity map

The flexural deformation beneath Pūhāhonu was estimated using a variable elastic thickness that depended on the age contrast between the seamounts and the seafloor (Watts, 2001). Because of uncertainties in this relationship (e.g., Watts, 2001), we let the nominal elastic thickness follow the depth to the 450 °C isotherm in a cooling plate model but bracketed the results with estimates obtained from using the 300 °C and 600 °C isotherms, thus covering the reported range of elastic thickness estimates globally (e.g., Watts and Zhong, 2000). Half the difference between the thickness estimates for these two temperatures was assigned as the uncertainty in the volume calculation of the compensation for the nominal 450 °C isotherm. Following Wessel (2016), Hawaiian Ridge age progression and crustal seafloor ages at Pūhāhonu yielded a plate age during Pūhāhonu construction of ~88 Myrs. Thus, we

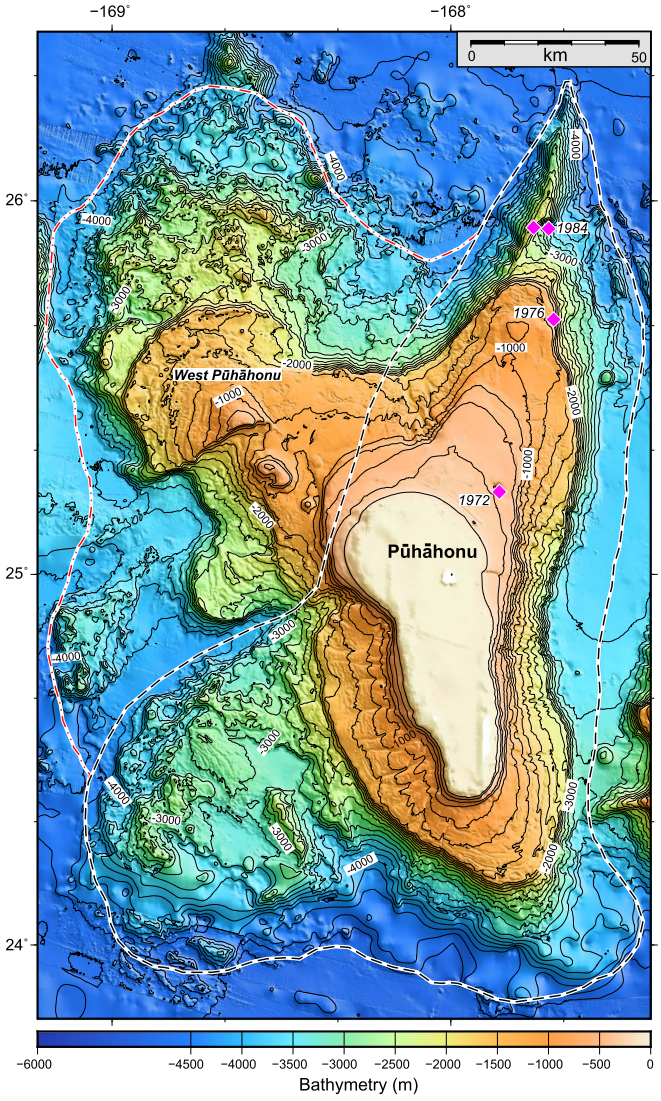

Fig. 2. Detailed bathymetric map of Pūhāhonu and West Pūhāhonu volcanoes. Magenta diamonds show the locations of the four dredge hauls that were collected on Pūhāhonu in 1972, 1976 and 1984. The samples collected in 1976 are olivine-rich and the focus of this study. The black dashed line shows the inferred boundary for Pūhāhonu that was used in the volume calculation. Note that this boundary is displaced 5-10 km to the east of the change in slope on Pūhāhonu's west rift zone to help compensate for the overlap with older West Pūhāhonu volcano. The red dash-dot line shows the inferred boundary of West Pūhāhonu volcano. The combined area of these two regions was used to calculate the total volume for comparison with the volume for the Island of Hawai'i.

estimated the nominal elastic thickness to be 29 ± 10 km. Our flexural calculations used this range of elastic thicknesses to estimate uncertainties in compensation volume to be ~20% (Fig. 4). Our nominal elastic thickness is significantly lower than the 40 km approximation inferred by Watts and ten Brink (1989) and used by Robinson and Eakins (2006) in their estimation of compensation volumes beneath the Hawaiian Islands. However, 40 km is likely an overestimate as Watts and ten Brink (1989) did not account for the long-wavelength influence of the Hawaiian swell topography (Zhong and Watts, 2013). Wessel (1993) reported a swell-corrected estimate of elastic thickness for the Hawaiian Islands of 33 km, which is closer to our nominal value. However, elastic thickness estimates for the dynamic setting of the volcanically active Island of Hawai'i may not directly be applicable to the long-relaxed tectonic setting of Pūhāhonu, hence our bracketing of observed elastic thicknesses for this load age using global trends (Watts, 2001) is a more conservative estimate.

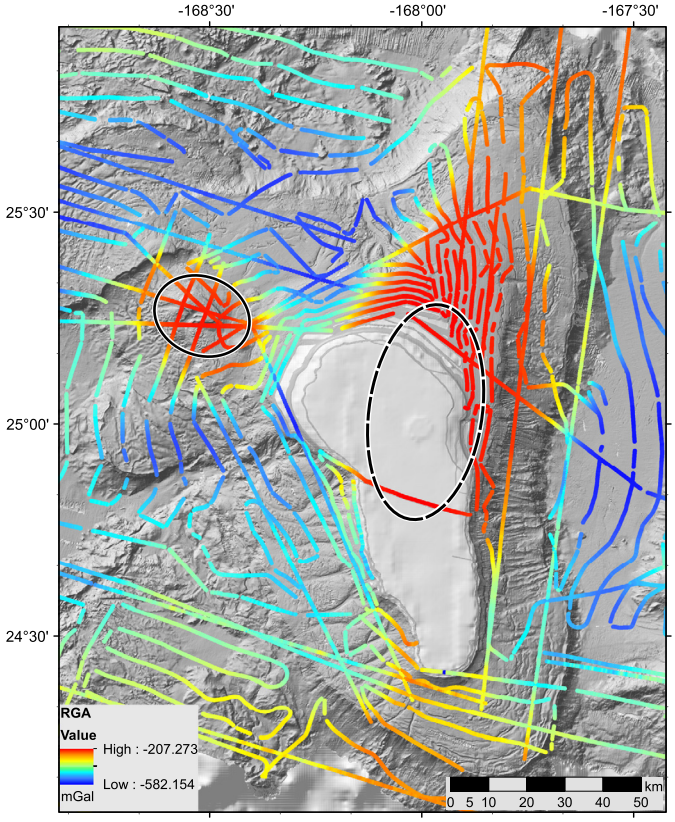

Fig. 3. Residual gravity anomalies along ship tracks of R/V *Falkor* and others (colored lines) overlain on bathymetry hillshade (gray background) as described for Fig. 2. Solid black ellipse is a gravity high interpreted as a volcanic center on West Pūhāhonu volcano and inferred where dashed on Pūhāhonu volcano due to lack of coverage over the large and relatively shallow carbonate bank.

The new gravity data was collected during the R/V *Falkor* cruises to the PMNM in 2014 (FK140307, FK140502) using a BGM-3 gravimeter. These data were merged with data from prior expeditions from the National Centers for Environmental Information (NCEI) including the GLORIA campaign (Paskevich et al., 2011) to map out residual gravity anomalies (Fig. 3). The Residual Gravity Anomaly (RGA) was calculated by subtracting the gravity due to a flexed lithosphere from the Bouguer gravity values. Thus, the RGA calculation is the final gravity reduction that illustrates density differences where cumulate core and dike complexes are located. The gravity data were used to identify the two volcanic centers in the Pūhāhonu area.

3.2. Olivine analyses and primitive mantle potential temperature calculations

The University of Hawai'i at Mānoa electron microprobe was used to make high precision olivine analyses. Conditions were 200 nA, 20 KeV and 10 µm beam diameter with 100 s counting time on the peak for Si, Mg, Ni, Ca, Mn and Fe, and 50 s on backgrounds on each side of the peak. High-intensity crystals were used to enhance count rates for Ni (LIFH) and Ca (PETH). Calibration standards were San Carlos olivine USNM 111312/444 (SiO_2, MgO, FeO), Verma Garnet (MnO), Kakanui Augite USNM 122142 (CaO), and a synthetic Ni-oxide (NiO). Raw X-ray intensities were converted into weight percent via ZAF corrections. Excellent reproducibility with the published Smithsonian values for the San Carlos and Springwater olivines was achieved with this calibration scheme (see Table A1).

Olivine liquid temperatures were calculated using the equation 4 thermometer of Putirka et al. (2007), with modifications as described below. The parental magma composition in equilibrium with the highest olivine forsterite content was calculated to determine the maximum $T^{ol\text{-}liq}$ recorded for the Pūhāhonu sample. The amount of Fe_2O_3 in the melt was calculated assuming an oxygen fugacity of QFM-1 using the model of Kress and Carmichael (1988). Calculations were made under isobaric conditions of 1 kbar (~3 km), a reasonable depth for Hawaiian tholeiitic magma reservoirs based on observations for the active volcanoes Mauna Loa and Kīlauea (Poland et al., 2014). All olivine cores used in parental magma calculations have CaO $\geq$0.17 wt.%, indicating that they are magmatic in origin and not mantle xenocrysts, which typically have <0.1 wt.% CaO (e.g., Larson and Pederson, 2000).

One major assumption in reconstructing parental magma compositions is that the K_d value is constant during the evolution of the magma. However, K_d is compositionally dependent and not constant during fractionation (e.g., Toplis, 2005). To evaluate the magnitude of this variable on our compositions, K_d was recalculated following each iterative step of the parental magma calculation using the equation of Toplis (2005). Parental magma compositions were estimated using Petrolog V3.1.1.3 (Danyushevsky and Plechov, 2001) to equilibrate with the highest Fo olivine in the six analyzed samples. Small weight fractions (0.01 wt.%) of the median Fo olivine composition was removed or added to the XRF whole-rock composition. This process was iterated until the parental magma Mg# was in equilibrium with the highest Fo measured within each sample. The same parameterization was used for all other variables and K_d was allowed to vary. This method yielded similar final K_d values that are in agreement with the K_d=0.345±0.030 assumption used here from the work of Matzen et al. (2011) on Hawaiian basalts. This difference in final parental magma composition results in 20-25 °C difference in $T^{ol\text{-}liq}$. Thus, the $T^{ol\text{-}liq}$ values obtained using the compositionally-dependent K_d method are within the 2σ uncertainty of the constant K_d approach used here.

4. Results and interpretation

4.1. Geologic interpretations of the new bathymetric and gravity maps

Extensive multibeam surveys in the PMNM were carried out aboard R/V *Falkor* in 2014 using the hull mounted Kongsberg EM 302 and EM 710 sonars. We added these data to the existing bathymetric synthesis for the NWHR, along with a version fusing all the multibeam data with the lower resolution SRTM15+V2 global bathymetry and topography data set (Tozer et al., 2019) at a grid cell interval of 60 m. This bathymetric synthesis reveals that Pūhāhonu has an immense and complex morphology belied by the two, tiny volcanic pinnacles that are the only subaerial remnants of this once enormous shield volcano.

The basic structure of Pūhāhonu volcano is delineated by its recently collected and compiled bathymetry and marine gravity data (Figs. 2 and 3). Pūhāhonu is massive; ~275 km long and ~90 km wide (Fig. 2). Two broad, very long rift zones are evident in the bathymetry data; one extending ~140 km to the south with a kink to the east at ~1000 m water depth, and another extending 150 km to the north. The north rift abruptly narrows below 2000 m water depth with a sharp break in slope that probably marks the old shoreline formed near the end of Pūhāhonu's shield stage as discussed further below. Both rifts extend to water depths of at least 4500 m. These rift zones are comparable in length and width to the longest rift in the Hawaiian Islands (Haleakalā's east rift zone, 160 km long and 30-40 km wide to depths of ~2000 m; Fig. 1). The breadth of the Pūhāhonu and Haleakalā rifts probably reflects the subaerial growth of these volcanoes and the later formation of a carbonate cap as these volcanoes subsided below

sea level. A bulbous, ~50 km long and wide ridge trends northwestward from Pūhāhonu's summit high and probably represents a third rift zone (Fig. 2).

The gravity data over the north rift show that it has a well-defined residual gravity high (Fig. 3; see Methods for detail on anomaly formulation). The other two rifts were poorly surveyed for gravity because of the shallow water depths of the summit carbonate platform. Sixty kilometers west of Pūhāhonu is another residual gravity high anomaly underlying an 800 m bathymetric high (Fig. 3). We interpret this feature as the summit of a separate volcanic center given its bathymetric complexity and size, the substantial gravity high and its ~60 km spacing from the summit of Pūhāhonu (Figs. 2 and 3). This spacing is typical of the average interval between volcanic centers along the NWHR (~57 km), although there is also considerable variation in volcano spacing (16-175 km; Garcia et al., 2015). A map by Jackson et al. (1972) first identified this bathymetric high as a separate volcano, although it remained unnamed (Garcia et al., 2015). Here we refer to it as West Pūhāhonu (Fig. 2).

Pūhāhonu volcano is capped by an expansive carbonate bank extending from <50 m to ~800 m water depth (Fig. 2). Another prominent feature in the new bathymetry map is a marked slope break, which in the Hawaiian Islands is thought to signify the shoreline near the end of the shield stage (marking the maximum size of the subaerial volcano; e.g., Moore, 1987). The slope break reflects the shallower, gentle slopes formed by subaerial lava flows, whereas the steeper slopes are formed by submarine flows as they are rapidly quenched (e.g., Moore, 1987). The depth of this slope break varies dramatically across Pūhāhonu (Fig. 2). It is relatively shallow on the distal ends of the north rift (~1200 m) and south rift zone (~1500 m) but much deeper on the east flank of the summit (~2300 m). However, the slope break is at ~1700 m on the west flank of the summit (Fig. 2). The remarkable variation in depth of this break probably reflects the rapid loading of the lithosphere by Pūhāhonu volcano (sinking more rapidly in the center) and tilting to the east as a consequence of the loading by the younger volcano (St. Rogatien) to the southeast. The new bathymetry map also illustrates the size and extent of a large slump deposit on the southwest flank of Pūhāhonu (Fig. 2). Large slumps are a common feature on Hawaiian shield volcanoes (Moore et al., 1994). This landslide has several 25 km long blocks extending up to 65 km from the break in slope on the southwest flank of Pūhāhonu (Fig. 2).

4.2. How massive is Pūhāhonu?

The edifice volume of Pūhāhonu was derived from the difference between the relief and the best approximation for the Hawaiian swell, which was estimated using an optimal robust separator filter (e.g., Wessel, 2016). The subsurface volume was approximated assuming flexural compensation of the edifice (Fig. 4), following the approach of Wessel (2016; see Methods for details). Unlike previous estimates of volcanic volumes for the Hawaiian Islands that incorporate estimates of the compensation volume, our calculations are the first to include realistic uncertainties. Because the swell model also has formal uncertainties, both sets of uncertainties contribute to the total volume uncertainty. The total eruptive volume of Pūhāhonu is thus the sum of the edifice and compensation volumes with combined uncertainties of ~20%.

The Pūhāhonu volume was computed with a vertical boundary between its west rift and West Pūhāhonu volcano (Fig. 2). The extent of the overlap of the two volcanoes at depth is unknown. Therefore, the boundary for the volume calculation was shifted 5-10 km eastward of the topographic surface boundary (based on change in slope) to help compensate for the overlap of the two volcanoes (Fig. 2). The total edifice volume (above the ocean floor is $49 \pm 11 \times 10^3$ km^3 whereas the subsurface volume is $100 \pm 27 \times 10^3$ km. The resulting volume for Pūhāhonu volcano is $148 \pm 29 \times 10^3$ km^3. This estimate does not include the volcanoclastic fill in the moat surrounding the volcano that was probably derived from Pūhāhonu. Hence, this is a conservative estimate of Pūhāhonu's volume. The carbonate cap on Pūhāhonu is estimated to contribute $\sim 2.2 \times 10^3$ km^3, assuming the thickness is ~400 m as found on Midway (Ladd et al., 1970), the only area in the NWHR that has been drilled to evaluate the carbonate thickness. This is less than 10% of the error for our volume calculation (29×10^3 km^3, or 19% uncertainty based on the square root of the sum of squared errors).

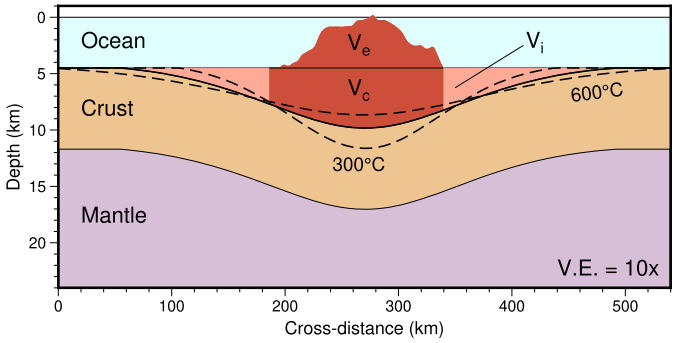

Fig. 4. The eruptive volume is approximated by the edifice component (V_e) above the surrounding seafloor (which is the swell model shape in our study) plus the volume beneath the edifice filling in the depression (V_c) caused by the flexural deformation. Because of unknown lateral interactions with neighboring West Pūhāhonu volcano, the contact was assumed to be vertical between the volcanoes. Also, no allowance was made for a sloping contact buried beneath the volcaniclastic infill (V_i). Neither the volcaniclastic moat fill (V_i), nor any or material ponded beneath the crust are included. Thus, this volume estimate is a conservative lower limit on the total volume of Pūhāhonu volcano. V.E. is vertical exaggeration. (Figure modified from Wessel, 2016).

The new volume calculation shows that Pūhāhonu is substantially larger than any other Hawaiian volcano including Mauna Loa, which was presumed to be the largest volcano on Earth (e.g., Lipman and Calvert, 2013). Recent volume calculations for Mauna Loa are 74.0×10^3 km^3 (Robinson and Eakins, 2006) and 83×10^3 km^3 (Lipman and Calvert, 2013). Neither of these calculations have error estimates. The higher of these two volumes assumed a too young age for the adjacent Kīlauea volcano (Garcia et al., 2017) resulting in a too large volume for Mauna Loa. Robinson and Eakins (2006) used a similar approach as employed here with vertical contacts between volcanoes and a volcano base defined by the seismic reflection imagery of Watts and ten Brink (1989). They found a depth to the oceanic crust under Mauna Loa of ~9 km, which is nearly identical to what we found for Pūhāhonu (Fig. 4). Using the more likely volume estimate of Robinson and Eakins (2006), Pūhāhonu volcano is about twice the size of Mauna Loa ($148 \pm 29 \times 10^3$ km^3 vs. 74.0×10^3 km^3).

An even larger shield volcano, Tamu Massif, was reported in the north Pacific basin, although a new study (Sager et al., 2019) found linear magnetic field anomalies with opposite magnetic polarity on the massif. Thus, Tamu is now interpreted to have formed as a result of voluminous, ridge-focused volcanism and not to be a single shield volcano (Sager et al., 2019). Thus, our new volume calculations establish Pūhāhonu as the largest shield volcano on Earth.

4.3. What caused Pūhāhonu's large volume?

Three testable mechanisms for the anomalous size of Pūhāhonu can be ruled out: 1.) Lithospheric thickness. A thinner, warmer lithosphere is needed to promote higher magmatic flux (e.g., White, 1993). The lithosphere under Pūhāhonu was formed in the

Cretaceous, and was relatively cold and thick at the time it formed (~80 Myr difference between lithosphere and volcano age; White, 1993; Jicha et al., 2018). In fact, all of the Hawaiian Ridge (from the HE Bend to the Island of Hawai'i) is underlain by lithosphere that is 80-90 Myrs older than the overlying Hawaiian volcano. Furthermore, there is no fracture zone under the volcano (Fig. 1) to allow shallower melting or higher magma flow rates (White, 1993). Thus, the dramatic variations in the volume flux along the Hawaiian Ridge cannot be related to the lithosphere thickness. 2.) Propagation rate. The rate for the southern section of the NWHR where Pūhāhonu is located was relatively fast (87 km/Ma; Jicha et al., 2018). All things being constant, a faster rate should lead to a smaller volcano similar to many of the other volcanoes along this section of the NWHR. Surprisingly, the older section of the NWHR (>25 Ma) formed a slower propagation rate (57 km/Myr; Jicha et al., 2018) but has more widely spaced, smaller volcanoes (Fig. 1). Thus, propagation rate has apparently played no role in governing the size of volcanoes along the Hawaiian Ridge. 3.) A more fertile source composition. The source for Pūhāhonu basalts (including samples from dredge haul 76-6-7 that were examined here) is Kea-like in composition for major and trace elements, and its lavas have Sr, Nd and Pb isotope ratios similar to those from other, much smaller volcanoes along this section of the NWHR (Harrison and Weis, 2018; Fig. 1). Thus, the Pūhāhonu source was not more fertile.

A fourth testable mechanism for enhanced magmatic flux is high melting temperature. Melt generation is highly sensitive to even small perturbations in a plume's thermal structure (e.g., White, 1993; Lee et al., 2009). The Hawaiian plume thermal structure has been geodynamically modeled using plume buoyancy flux models to predict the Hawaiian swell topography (e.g., Ribe and Christensen, 1999). This method approximates mantle potential temperatures (T_p) by solving for combinations of mass flux and plume temperature that minimize error in reproducing the swell shape. However, these solutions are non-unique, making it difficult to decouple the influences of mass flux from temperature and they ignore source fertility variations.

Olivine thermometry provides an alternative and more direct approach to estimate T_p (Putirka, 2016). Six Pūhāhonu picritic basalts (>15 vol.% olivine; Table A2) from the 1976 dredge haul (Fig. 2) were utilized here to investigate whether Pūhāhonu lavas were produced at higher temperatures. Whole-rock compositions were previously analyzed by XRF for major and trace elements (Garcia et al., 2015). These compositions lie along the same MgO-FeO trend as lavas from Kilauea and at a higher FeO value than those from Mauna Loa. The maximum olivine-liquid temperatures ($T^{ol\text{-}liq}$) were corrected for adiabatic decompression and heat of fusion to determine the T_p for the most primitive (i.e., highest forsterite, 100 [Mg/(Mg + Fe)], content) olivine from Pūhāhonu (see Methods for information on these calculations). High precision analyses (see Methods for details on analysis routine) were made for 331 olivine phenocrysts. Forsterite (Fo) contents of cores from euhedral olivine phenocrysts (many with melt inclusions that are indicative of crystallization in a melt; Fig. 5) from these basalts range from 91.85 to 87.3%, with most between 89-91% Fo (see Table A3 for highest Fo olivine from these basalts). The CaO contents of the highest Fo olivine are moderate (0.20-0.22 wt.%; Table A3) indicating they were formed by crustal depth crystallization from tholeiitic magma rather than being mantle xenocrysts (<0.10 wt.% CaO; e.g., Larson and Pederson, 2000). The highest Fo value (91.85%; Fig. 5) is significantly higher than the previous most forsteritic olivine ever reported for the Hawaiian-Emperor Chain (Mauna Loa, 91.3%; Garcia et al., 1995). Higher Fo olivine is indicative of hotter magma (Putirka, 2016).

A Monte Carlo simulation method was used to calculate olivine-liquid equilibration temperature ($T^{ol\text{-}liq}$) of the host magma, mantle potential temperature (T_p), and the uncertainties in temperature associated with equilibrium assumptions made for the estimate of the parental magma composition (see Table A4 for parental magma compositions for the six Pūhāhonu samples studied). Pressure was estimated using the Si-activity barometer of Putirka (2008).

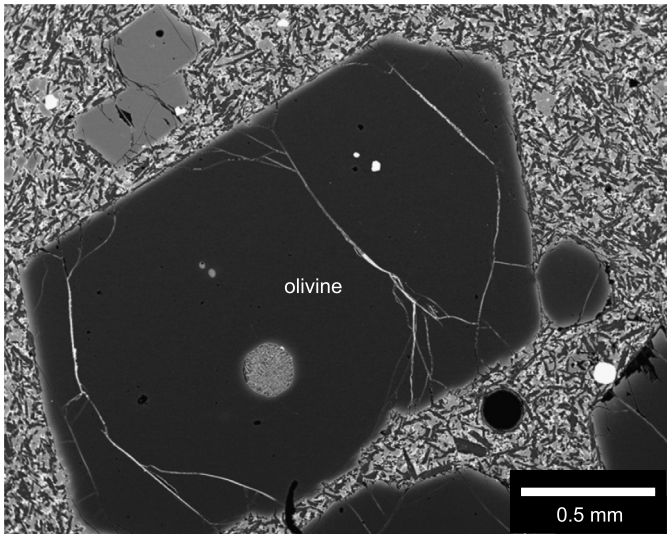

Fig. 5. Backscatter electron image of the Fo 91.85% olivine from sample 76-6-7-H. Note the euhedral morphology of the crystal, lack of alteration, apparent nearly uniform dark gray color (Fo 91.4-91.8%), the circular lighter gray melt inclusion and the sharp, iron-rich (lighter gray, Fo 82%) rim. Most of the phenocrysts in this thin section and others from this dredge haul are also high in Fo (89-91%, dark gray; lower right corner), although the two crystals in the upper left of this image are lighter gray (Fo 83%).

$$
\begin{aligned}
P\,(kbar) = {} & 231.5 + 0.186T^{ol-liq}\,(C^{\circ})\,0.124 \\
& + T^{ol-liq}\,(C^{\circ}) \ln\left(a^{liq}_{SiO_2}\right) - 528.5\left(a^{liq}_{SiO_2}\right)^{1/2} \\
& + 13.3\left(X^{liq}_{TiO_2}\right) + 69.9\left(X^{liq}_{NaO_{0.5}} X^{liq}_{KO_{0.5}}\right) \\
& + 77.3\left(\frac{X^{liq}_{AlO_{1.5}}}{X^{liq}_{AlO_{1.5}} + X^{liq}_{SiO_2}}\right)
\end{aligned}
$$

The percent melting was then calculated. This gave a pressure of 3.2 GPa and 24% melting for the Puhahonu basalt. Using these values, the T_p for the Fo 91.85% olivine is 1703 ± 56 °C (all temperature uncertainties are 2 sigma values). This is the highest T_p reported for any Hawaiian basalt but within the 2 sigma uncertainty for the value obtained for a Mauna Loa olivine with Fo 91.3% (T_p Hawaii = 1670 ± 51 °C; Putirka, 2016).

4.4. The pulsing Hawaiian plume

Magma productivity (melt flux) has been highly variable along the Hawaiian Ridge from the Bend in the Hawaiian-Emperor Chain to the Island of Hawai'i (Fig. 6). The flux was relatively low after the Bend (~ 0.5 $m^3\,s^{-1}$) producing small, widely spaced volcanoes (e.g., White, 1993; Clague, 1996; Wessel, 2016). Flux rate increased markedly to ~ 6 $m^3\,s^{-1}$ at 14-15 Ma when Pūhāhonu's shield formed and subsequently progressively decreased to moderate rates until after Middle Bank volcano was formed at the southeastern (younger) end of the NWHR (~ 2 $m^3\,s^{-1}$; Figs. 1 and 6). The Hawaiian Islands (starting at ~5 Ma) mark a second increase in melt flux that peaked at ~ 10 $m^3\,s^{-1}$ for the Island of Hawai'i when Mauna Loa was formed. Petrologic evidence presented above for Pūhāhonu and by Putirka (2016) for Mauna Loa indicates that an increase in plume temperature played an essential role in both

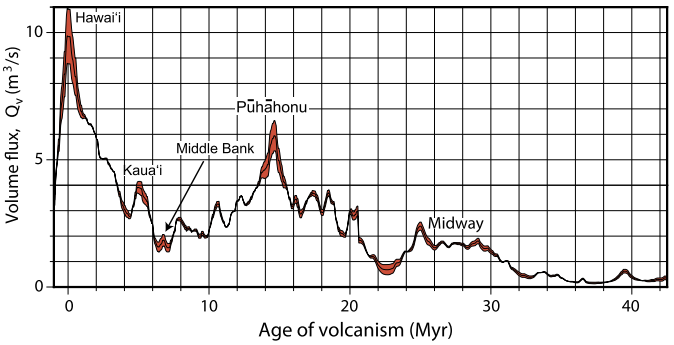

Fig. 6. Volume flux (m^3/s) versus eruption age (Myr) along the Hawaiian Ridge. The red band indicates the 1-sigma uncertainty in the flux estimates. Modified from Wessel (2016).

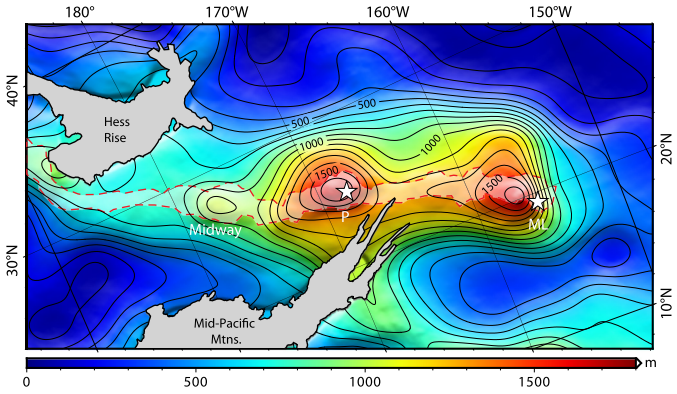

Fig. 7. Swell height estimates given by the regional-residual ORS separation of Wessel (2016). (Figure modified after Wessel (2016).)

of these magmatic flux pulses for the Hawaiian Ridge. These results support the original hypothesis of White (1993) that plume temperature was the main control on the magma flux variations along the Hawaiian Ridge.

The recent higher magmatic output for the Hawaiian Islands also involved a more fertile source, the Loa component (named for Mauna Loa). This source emerged as a prominent component for many Hawaiian Island volcanoes during formation of Kaua'i volcano (~5 Ma) (e.g., Williamson et al., 2019). Despite not having a more fertile source, the total volume of the Pūhāhonu and West Pūhāhonu two-volcano complex ($224 \pm 44 \times 10^3$ km^3) is nearly identical to the total volume estimated for the entire Island of Hawai'i with its seven volcanoes and its paired chain of volcanoes (213×10^3 km^3; Robinson and Eakins, 2006), although three of these volcanoes are still active (i.e., eruptions within the last 100 years). The higher magmatic flux at Pūhāhonu may have been short-lived (~3 Myrs) whereas the Hawaiian Islands pulse is longer-lived (≥5 Myrs), starting in the northern Hawaiian Islands and continuing on the Island of Hawai'i (Fig. 6). In addition to these two major pulses of increased magmatic output for the Hawaiian plume, a smaller pulse apparently occurred at 24-30 Ma as volume flux more than doubled (Fig. 6).

Thermal pulses are atypical for mantle plumes. Instead, many well studied mantle plume provinces (e.g., Reunion, Iceland, Galapagos) show evidence of secular cooling following formation of large igneous provinces (White, 1993; Herzberg and Gazel, 2009) or exhibit a marked decrease in magma flux along the chain (e.g., Louisville chain, Koppers et al., 2011). It has been argued that Paleocene to Permian mantle plumes were hotter and melted more extensively than the plumes forming modern ocean islands (Herzberg and Gazel, 2009). This has been attributed to the overall thermal decline of the Earth (e.g., Putirka, 2016). However, the decrease in T_p for the Iceland plume may have been only ~50 °C (Hole and Millett, 2016).

The Hawaiian mantle plume is an exception to the general secular cooling trend as was noted by many previous studies (e.g., White, 1993; Herzberg and Gazel, 2009; Putirka, 2016). The petrologic results demonstrate that the two sharp increases in magma flux along the Hawaiian Ridge in the last 15 Myrs (Fig. 6) are related to relatively short-term thermal pulses. These magmatic pulses are also geophysically reflected in the height of the swell related to the Hawaiian plume, which shows two marked peaks near Pūhāhonu and Mauna Loa volcanoes (Fig. 7). Furthermore, the maximum T_p for Pūhāhonu and Mauna Loa (~1700 and 1670 °C) are even higher than those estimated for the Cretaceous Deccan Traps and North Atlantic flood basalts (up to 1640 °C; Herzberg and Gazel, 2009).

Pulsations in mantle plume magmatism may result from fluctuations in core-mantle interaction involving periodic heating of Earth's core (e.g., Nakagawa and Tackley, 2005) that create increased plume activity along the edges of the lower-mantle anomalies (Burke et al., 2008). Global seismological tomography studies have discovered two large, anomalously slow areas under Africa and the central Pacific, which are interpreted as upwellings spanning the entire depth of the mantle (e.g., Garnero et al., 2016). Hawai'i and the majority of longer-lived hotspots are located near the edges of these lower-mantle low-velocity anomalies (e.g., Burke et al., 2008) suggesting that hotspots are the surface expressions of mantle plumes originating from the deepest mantle. The notable feature of the thermal pulse that formed Pūhāhonu volcano is that it was short-lived (2-3 Myrs) and didn't involve a geochemically enriched source. In contrast, the high volume flux that produced the Hawaiian Islands included the fertile Loa source component (e.g., Williamson et al., 2019).

Mirroring the plume flux (Fig. 7), the swell amplitude also has peaks near Pūhāhonu and Mauna Loa volcanoes (white stars). Lighter shaded area with dashed red outline indicates the Hawaiian Ridge. The Mesozoic Hess Rise and Mid-Pacific Mountains (gray) were excluded from the regional-residual modeling.

A solitary wave is an alternative and complementary explanation for the immense size and the high degree of melting estimated for some Pūhāhonu basalt (24%). Solitary waves are stable ascending blobs of buoyant, viscous mantle created by perturbations in the flux entering the conduit (Scott et al., 1986). Fluctuations in volume flux along the trails of many plumes including Iceland (Ito, 2001), Azores (Escartin et al., 2001) and Hawai'i (e.g., White, 1993) have been attributed to solitary waves almost entirely based on fluctuations in volume flux. The petrologic results for Pūhāhonu demonstrate that a thermal pulse played a key role in its large volume. A solitary wave would widen the plume diameter allowing the core of the rising hot plume to be better insulated yielding hotter magma and higher extents of melting (e.g., White, 1993; Ito, 2001; Ribe et al., 2007). Thus, a solitary wave would be an excellent mechanism for creating the enormous size and high temperature basalt found at Pūhāhonu.

5. Conclusions

New bathymetric mapping, refined volume calculations and petrologic analyses were presented for Pūhāhonu, a ~12-14 Ma volcano in the northwest Hawaiian Ridge.

1. These results show that Pūhāhonu is the largest shield volcano on Earth. It is twice the size of Mauna Loa volcano (148 ± 29 vs. 74.0×10^3 km^3), which was assumed to be not only the largest Hawaiian volcano but also the largest known shield volcano on Earth.

2. Three testable mechanisms were considered and rejected as the cause of Pūhāhonu's enormous size. The lithosphere was too

thick and cold to allow for greater extents of partial melting when Pūhāhonu was formed, and the propagation rate was relatively fast (87 km/Myr) when it formed. Furthermore, the source for Pūhāhonu basalts was Kea-like and no more fertile than for other much smaller NWHR volcanoes. Thus, these are unlikely reasons for the great size of this volcano.

3. Pūhāhonu tholeiitic basalts contain high forsteritic content olivine including the highest value ever measured for a Hawaiian basalt (Fo 91.85%). Calculations of the mantle potential temperature based on this high forsterite olivine indicated that magma temperatures were high (∼1700 °C) and greater than any Hawaiian basalt. Thus, the gargantuan size of Pūhāhonu reflects its high melting temperature, the highest reported for any Cenozoic basalt.

4. The Hawaiian plume has had two major magmatic flux pulses: one that produced the Hawaiian Islands, and the other that formed Pūhāhonu and West Pūhāhonu volcanoes. The high magmatic flux for the Hawaiian Islands is in part related to a more fertile source (the Loa component) whereas the source for Pūhāhonu basalts was not enriched.

5. A solitary wave within the Hawaiian plume is the probable cause of Pūhāhonu's higher melting temperature, high degree of partial melting and the resulting increased volume flux without invoking the need for an enriched source. A solitary wave would widen the plume diameter allowing the core of the rising hot plume to be better insulated yielding hotter magma and higher extents of melting.

The Hawaiian-Emperor Chain is arguably the world's best studied surface expression of a mantle plume. Nonetheless, new insights into its magmatic and thermal history continue to be revealed as more of the Hawaiian-Emperor Chain is mapped and sampled. These insights are providing a more complete understanding of the mechanics and thermal evolution of mantle plumes.

Declaration of competing interest

The authors declare that they have no known competing financial interests or personal relationships that could have appeared to influence the work reported in this paper.

Acknowledgements

The authors thank Fris Campbell, David Clague, Garrett Ito and Sandy Shor for discussions and/or help with obtaining samples from the University of Hawai'i rock storage facility, Michael Vollinger for XRF analyses, Lauren Froberg and Lerma Gamiao for assistance with sample preparation, and Keith Putirka and an anonymous reviewer for their comments on the manuscript. The captains, crews, and science team members of R/V *Falkor* cruises FK140307 and FK140502 are thanked for their expertise in making these expeditions successful. Ship time support to Christopher Kelley and J.S. was provided by Schmidt Ocean Institute. M.G. and J.T. were supported by NSF grant EAR-1219955; M.G., P.W. and J.S. by NSF grant OCE-1834758; J.S. and J.T. by NSF grant OCE-1558445. This paper is SOEST Contr. #10974.

Appendix A. Supplementary material

Supplementary material related to this article can be found online at https://doi.org/10.1016/j.epsl.2020.116296.

References

Bargar, K.E., Jackson, E.D., 1974. Calculated volumes of individual shield volcanoes along the Hawaiian-Emperor chain. J. Res. U.S. Geol. Surv. 2, 545–550.

Burke, K.C., Steinberger, B., Torsvik, T., Smethurst, M.A., 2008. Plume generation zones at the margins of large low shear velocity provinces on the core–mantle boundary. Earth Planet. Sci. Lett. 265, 49–60.

Clague, D.A., 1996. The growth, subsidence of the Hawaiian-Emperor volcanic chain. In: Keast, A., Miller, S.E. (Eds.), The Origin and Evolution of Pacific Island Biotas, New Guinea to Eastern Polynesia: Patterns and Processes. SPB Academic Publishing, Amsterdam, pp. 35–50.

Clapp, R.B., 1972. The natural history of Gardner Pinnacles, Northwest Hawaiian Islands. Atoll Res. Bull. 163, 1–31.

Dalrymple, G.B., Lanphere, M.A., Jackson, E.D., 1974. Contributions to the petrography and geochronology of volcanic rocks from the leeward Hawaiian Islands. Geol. Soc. Am. Bull. 85, 727–738.

Danyushevsky, L.V., Plechov, P., 2001. Petrolog3: integrated software for modeling crystallization processes. Geochem. Geophys. Geosyst. 12, Q07021. https://doi.org/10.1029/2011GC003516.

Escartin, J., Cannat, M., Pouliquen, G., Rabain, A., Lin, J., 2001. Crustal thickness of V-shaped ridges South of the Azores: interaction of the Mid-Atlantic Ridge (36°–39°N) and the Azores hot spot. J. Geophys. Res. 106, 21,719–21,735.

Garcia, M.O., Grooms, D.G., Naughton, J.J., 1987. Petrology and geochronology of volcanic rocks from seamounts along and near the Hawaiian ridge: implications for propagation rate of the ridge. Lithos 20, 323–336.

Garcia, M.O., Hulsebosch, T., Rhodes, J., 1995. Olivine-rich submarine basalts from the southwest rift zone of Mauna Loa Volcano: implications for magmatic processes and geochemical evolution. In: Mauna Loa Decade Volcano. In: Am. Geophys. Un. Mono., vol. 92, pp. 219–239.

Garcia, M.O., Smith, J.R., Tree, J.P., Weis, D., Harrison, L., Jicha, B.R., 2015. Petrology, geochemistry, and ages of lavas from Northwest Hawaiian Ridge volcanoes. In: Neal, C.R., Sager, W., Sano, T., Erba, E. (Eds.), The Origin, Evolution, and Environmental Impact of Oceanic Large Igneous Provinces. In: Geological Society of America Special Paper, vol. 511, pp. 1–26.

Garcia, M.O., Jicha, B.R., Marske, J.P., Pietruszka, A.J., 2017. How old is Kīlauea Volcano? Insights from $^{40}Ar/^{39}Ar$ dating of the 1.7-km-deep SOH-1 core. Geology 45, 79–82.

Garnero, E.J., McNamara, A.K., Shim, S.-H., 2016. Continent-sized anomalous zones with low seismic velocity at the base of the Earth's mantle. Nat. Geosci. 9, 481–489.

Harrison, L.N., Weis, D., 2018. The size and emergence of geochemical heterogeneities in the Hawaiian mantle plume constrained by Sr-Nd-Hf isotopic variation over ∼47 million years. Geochem. Geophys. Geosyst. 19. https://doi.org/10.1029/2017GC007389.

Herzberg, C., Gazel, E., 2009. Petrological evidence for secular cooling in mantle plumes. Nature 458, 619–622.

Hole, M.J., Millett, J.M., 2016. Controls of mantle potential temperature and lithospheric thickness on magmatism in the North Atlantic Igneous Province. J. Petrol. 57, 417–436.

Ito, G., 2001. Reykjanes 'V'-shaped ridges originating from a pulsing and dehydrating mantle plume. Nature 411, 681–684.

Jackson, E.D., Silver, E.A., Dalrymple, G.B., 1972. Hawaiian-Emperor chain and its relation to Cenozoic circumpacific tectonics. Geol. Soc. Am. Bull. 83, 601–618.

Jicha, B., Garcia, M.O., Wessel, P., 2018. Mid-Cenozoic Pacific plate motion change: Implications for the Northwest Hawaiian Ridge and circum-Pacific. Geology 46, 1–4.

Kelley, C., et al., 2015. New insights from seafloor mapping of a Hawaiian marine monument. Eos 96. https://doi.org/10.1029/2015EO030235.

Koppers, A.A.P., et al., 2011. New $^{40}Ar/^{39}Ar$ age progression for the Louisville hot spot trail and implications for inter–hot spot motion. Geochem. Geophys. Geosyst. 12, Q0AM02. https://doi.org/10.1029/2011GC003804.

Kress, V.C., Carmichael, I.S.E., 1988. The compressibility of silicate liquids containing Fe_2O_3 and the effect of composition, temperature, oxygen fugacity and pressure on their redox states. Contrib. Mineral. Petrol. 108, 82–92.

Ladd, H.S., Tracey, J.I., Gross, M.G., 1970. Deep drilling on Midway atoll: geology of the Midway area Hawaiian Islands. U. S. Geol. Surv. Prof. Pap. 680-A, 1–29.

Larson, L.M., Pederson, A.K., 2000. Processes in High-Mg, High-T magmas: evidences from olivine, chromite and glass in Paleogene picrites from West Greenland. J. Petrol. 41, 1071–1098.

Lee, C.-T.A., et al., 2009. Constraints on the depths and temperatures of basaltic magma generation on Earth and other terrestrial planets using new thermobarometers for mafic magmas. Earth Planet. Sci. Lett. 279, 20–33.

Lipman, P.W., Calvert, A.T., 2013. Modeling volcano growth on the Island of Hawaii: deep-water perspectives. Geosphere 9, 1348–1383.

Matzen, A.K., Baker, M.B., Beckett, J.R., Stopler, E.M., 2011. Fe-Mg partitioning between olivine and high-magnesium melts and the nature of Hawaiian parental liquids. J. Petrol. 52, 1243–1263.

Moore, J.G., 1987. Subsidence of the Hawaiian Ridge. U. S. Geol. Surv. Prof. Pap. 1350, 85–100.

Moore, J.G., Normark, W.R., Holcomb, R.T., 1994. Giant Hawaiian underwater landslides. Science 264, 46–47.

Morgan, W.J., 1971. Convection plumes in the lower mantle. Nature 230, 42–43.

Nakagawa, T., Tackley, P.J., 2005. Deep mantle heat flow and thermal evolution of the Earth's core in thermochemical multiphase models of mantle convection. Geochem. Geophys. Geosyst. 6 (8). https://doi.org/10.1029/2005GC000967.

Paskevich, V.F., et al., 2011. GLORIA sidescan-sonar imagery for parts of the U.S. Exclusive Economic Zone and adjacent areas. U.S. Geol. Surv. Open-File Rept. 2010-1332.

Poland, M.P., Miklius, A., Montgomery-Brown, E.K., 2014. Magma supply, storage, and transport at shield-stage Hawaiian volcanoes. U. S. Geol. Surv. Prof. Pap. 1801, 179–235.

Putirka, K., 2008. In: Putirka, K.D., Tepley, F. (Eds.), Thermometers and Barometers for Volcanic Systems. In: Rev. in Mineral. Geochem., vol. 69, pp. 61–120.

Putirka, K., 2016. Cooling rates and mantle potential temperatures (Tp) for Earth, Moon, Mars and Vesta, from new models for Tp, oxygen fugacity, ferric-ferrous ratios, and olivine-liquid Fe-Mg exchange. Am. Mineral. 101, 819–840.

Putirka, K., Perfit, M., Ryerson, F.J., Jackson, M.G., 2007. Ambient and excess mantle temperatures, olivine thermometry, and active vs. passive upwelling. Chem. Geol. 241, 177–206.

Ribe, N.M., Christensen, U.R., 1999. The dynamical origin of Hawaiian volcanism. Earth Planet. Sci. Lett. 171, 517–531.

Ribe, N.M., Davaukkem, A., Christensen, U.R., 2007. Fluid dynamics of mantle plumes. In: Ritter, J.R.R., Christensen, U.R. (Eds.), Mantle Plumes - A Multidisciplinary Approach. Springer, Berlin, pp. 1–48.

Robinson, J.E., Eakins, B.W., 2006. Calculated volumes of individual shield volcanoes at the young end of the Hawaiian ridge. J. Volcanol. Geotherm. Res. 151, 309–317.

Sager, W.W., et al., 2019. Oceanic plateau formation by seafloor spreading implied by Tamu Massif magnetic anomalies. Nat. Geosci. 12, 661–666.

Scott, D.R., Stevenson, D.J., Whitehead Jr., J.A., 1986. Observations of solitary waves in a viscously deformable pipe. Nature 319, 759–761.

Toplis, M.J., 2005. The thermodynamics of iron and magnesium partitioning between olivine and liquid: criteria for assessing and predicting equilibrium in natural and experimental systems. Contrib. Mineral. Petrol. 149, 22–39.

Tozer, B., et al., 2019. Global bathymetry and topography at 15 arc seconds: SRTM15+. Earth Space Sci. 6. https://doi.org/10.1029/2019EA000658.

Watts, A.B., 2001. Isostasy and Flexure of the Lithosphere. Cambridge University Press, Cambridge. 458 pp.

Watts, A.B., ten Brink, U.S., 1989. Crustal structure, flexure, and subsidence history of the Hawaiian Islands. J. Geophys. Res. 94, 10,473–410,500.

Watts, A.B., Zhong, S., 2000. Observations of flexure and the rheology of oceanic lithosphere. Geophys. J. Int. 142, 855–875.

Wessel, P., 1993. A reexamination of the flexural deformation beneath the Hawaiian Islands. J. Geophys. Res. 98, 12,177–112,190.

Wessel, P., 2016. Regional–residual separation of bathymetry and revised estimates of Hawaii plume flux. Geophys. J. Int. 204, 932–947.

White, R.S., 1993. Melt production rates in mantle plumes. Philos. Trans. R. Soc. Lond. Ser. A 342, 137–153.

Williamson, N., Weis, D., Scoates, J., Pelletier, H., Garcia, M.O., 2019. Tracking the geochemical transition between the Kea-dominated Northwest Hawaiian Ridge and the bilateral Loa-Kea trends of the Hawaiian Islands. Geochem. Geophys. Geosyst. 20, 4354–4369. https://doi.org/10.1029/2019GC008451.

Zhong, S., Watts, A.B., 2013. Lithospheric deformation induced by loading of the Hawaiian Islands and its implications for mantle rheology. J. Geophys. Res. 118, 6025–6048.